Plant Physiology, April 2000, Vol. 122, pp. 1343–1353, www.plantphysiol.org © 2000 American Society of Plant Physiologists

Subcellular Localization and Speciation of Nickel in Hyperaccumulator and Non-Accumulator *Thlaspi* Species[1]

Ute Krämer, Ingrid J. Pickering, Roger C. Prince, Ilya Raskin, and David E. Salt*

Fakultät für Biologie-W 5, Universität Bielefeld, 33615 Bielefeld, Germany (U.K.); Stanford Synchrotron Radiation Laboratory, Stanford University, Stanford Linear Accelerator Center, Stanford, California 94309 (I.J.P.); Exxon Mobile Research and Engineering, Annandale, New Jersey 08801 (R.C.P.); Biotech Center, Cook College, Rutgers University, New Brunswick, New Jersey 08903 (I.R.); and Chemistry Department, Northern Arizona University, Flagstaff, Arizona 86011 (D.E.S.)

The ability of *Thlaspi goesingense* Hálácsy to hyperaccumulate Ni appears to be governed by its extraordinary degree of Ni tolerance. However, the physiological basis of this tolerance mechanism is unknown. We have investigated the role of vacuolar compartmentalization and chelation in this Ni tolerance. A direct comparison of Ni contents of vacuoles from leaves of *T. goesingense* and from the non-tolerant non-accumulator *Thlaspi arvense* L. showed that the hyperaccumulator accumulates approximately 2-fold more Ni in the vacuole than the non-accumulator under Ni exposure conditions that were non-toxic to both species. Using x-ray absorption spectroscopy we have been able to determine the likely identity of the compounds involved in chelating Ni within the leaf tissues of the hyperaccumulator and non-accumulator. This revealed that the majority of leaf Ni in the hyperaccumulator was associated with the cell wall, with the remaining Ni being associated with citrate and His, which we interpret as being localized primarily in the vacuolar and cytoplasm, respectively. This distribution of Ni was remarkably similar to that obtained by cell fractionation, supporting the hypothesis that in the hyperaccumulator, intracellular Ni is predominantly localized in the vacuole as a Ni-organic acid complex.

Metal hyperaccumulator plants accumulate high concentrations of metals and metalloids such as Ni, Zn, and Se in aboveground tissues. In contrast, most other plants adapted to metal-rich soils exclude metals from the shoot (Shrift, 1969; Baker and Brooks, 1989). The genetic traits that determine this metal hyperaccumulation phenotype clearly offer the potential for development of practicable phytoremediation technologies (Chaney, 1983; Salt et al., 1998). However, although some progress has been made, the molecular basis underlying the hyperaccumulation process is not well understood (Salt and Krämer, 1999).

It has been suggested that metal hyperaccumulation may in part be determined by higher rates of metal translocation from roots to shoots. This appears to be true for Zn hyperaccumulation in *Thlaspi caerulescens* J. & C. Presl. (Lasat et al., 1996). However, rates of Ni translocation in the Ni hyperaccumulator *Thlaspi goesingense* Hálácsy and the non-accumulator *Thlaspi arvense* L. are very similar (Krämer et al., 1997). Instead, it appears that it is primarily the extraordinary degree of Ni tolerance in *T. goesingense* that allows this plant to accumulate Ni so effectively. Leaf protoplasts of *T. goesingense* were found to be more tolerant to Ni than those isolated from *T. arvense*, suggesting the existence of a Ni tolerance mechanism operating at the cellular level in the leaves of the hyperaccumulator (Krämer et al., 1997). However, the basis of this Ni tolerance mechanism was not determined.

There is some evidence that vacuolar localization may be associated with metal detoxification in plants (Krotz et al., 1989; Vögeli-Lange and Wagner, 1990; Brune et al., 1994, 1995). Vacuolar accumulation of Ni is essential for Ni resistance in the yeast *Saccharomyces cerevisiae* (Ramsay and Gadd, 1997; Nishimura et al., 1998). This vacuolar accumulation of Ni is driven by the pH gradient that exists across the vacuolar membrane of yeast (Nishimura et al., 1998). Surprisingly, this type of pH-gradient-dependent Ni transport could not be observed in roots of Ni-sensitive oat seedlings (Gries and Wagner, 1998), and only a minor accumulation of Ni could be detected in vacuoles isolated from leaves of Ni-sensitive barley (Brune et al., 1995). These results suggest that Ni-sensitive plants are not able to efficiently compartmentalize Ni within the vacuole. However, the compartmentalization of Ni in Ni-tolerant plants such as the Ni hyperaccumulator *T. goesingense* has not yet been investigated.

By isolating intact vacuoles from the Ni-tolerant hyperaccumulator *T. goesingense* and the Ni-sensitive non-accumulator *T. arvense*, we have been able to directly address the role of vacuolar Ni storage in cellular Ni tolerance. Using x-ray absorption spectroscopy we have also been able to non-invasively acquire information on the speciation of Ni in both hyper- and non-accumulator species. With this technique the ligand environment of metals

[1] This research was supported by a North Atlantic Treaty Organization fellowship awarded to U.K. by the German Academic Exchange Service (DAAD), by the U.S. Department of Energy (grant no. DE–FG07–96ER20251 to D.E.S.), and by Phytotech Inc. (to I.R.). Stanford Synchrotron Radiation Laboratory is funded by the Department of Energy, Office of Basic Energy Sciences (contract no. DE–AC03–76SF00515). The SSRL Structural Molecular Biology Program is supported by the National Institutes of Health, National Center for Research Resources, Biomedical Technology Program, and the Department of Energy, Office of Biological and Environmental Research.

* Corresponding author; e-mail david.salt@nau.edu; fax 520–523–8111.

can be probed in frozen tissues, minimizing any preparative steps and thus avoiding artifactual changes in metal complexation. Several research groups have recently started to exploit the advantages of this technique by investigating the speciation of Cd (Salt et al., 1995, 1997), Ni (Krämer et al., 1996), Zn (Salt et al., 1999), Cr (Lytle et al., 1998), Se (De Souza et al., 1998; Orser et al., 1999; Pilon-Smits et al. 1999), and As (Pickering et al., 2000) in plant tissues. Based on established information on pH and the composition of some cellular compartments in plants, it can be predicted that different, and in some cases compartment-specific, types of ligands will preferentially chelate Ni. Therefore, the quantitative speciation of a metal between a number of ligands allows a tentative estimate of the quantitative compartmentalization of this metal. In our experiments, the x-ray absorption spectroscopy data independently confirm the results obtained using the more invasive technique of tissue and cellular fractionation.

MATERIALS AND METHODS

Plant Cultivation

Seeds of *Thlaspi arvense* L. were obtained from the Research Station, Agriculture and Agri-Food Canada (Saskatoon, Canada). Seeds of *Thlaspi goesingense* Hálácsy were collected on an ultramafic site at Redschlag, Austria (Krämer et al., 1997). Seeds were germinated on filter paper moistened with 2.8 mM $Ca(NO_3)_2$ for 1 week and subsequently transferred into hydroponic culture as described previously (Krämer et al., 1997). Plants were cultivated in a growth chamber with 12-h light periods, during which plants were illuminated by a combination of fluorescent and incandescent light at a light intensity of 20,800 lux, and were maintained at day/night temperatures of 22°C/18°C and day/night humidities of 40%/50%. Exposure of plants to Ni was initiated 11 weeks and 8 weeks after germination for *T. goesingense* and *T. arvense*, respectively, to obtain plants of equivalent size.

Ni Exposure and Harvest

For the 1-week exposures, one specimen of *T. goesingense* was transferred into 0.4 L of aerated hydroponic solution supplemented with 10 μM $NiSO_4$ and 20 μCi of $^{63}NiCl_2$. Plants were exposed to Ni for 7 d with one replacement of the solution after 4 d. For the 1-d exposures, one plant of either *T. goesingense* or *T. arvense* was transferred into 0.4 L of aerated hydroponic solution containing 1 μM $NiSO_4$ and 40 μCi of $^{63}NiCl_2$ for 25.5 h. Approximately 2.5 g (fresh biomass) of fully expanded leaves was harvested from the plant with a razor blade at night. Quadruplicate samples of small leaf sections were cut from randomly selected leaves for Ni analysis. Small sections were pooled from several leaves for chlorophyll determinations and enzyme assays and frozen at −20°C until use. The remaining leaves were used for the isolation of protoplasts and vacuoles. For x-ray absorption spectroscopy studies, both *Thlaspi* species were grown as described above. A total of eight plants were transferred into 12 L of aerated hydroponic solution supplemented with 10 μM $NiSO_4$, and exposed to Ni for 7 d with one replacement of the solution after 4 d. Plants were harvested, separated into root and shoot tissues, and immediately frozen in liquid nitrogen. Frozen tissue was stored at −80°C, and then shipped frozen to the SSRL on dry ice.

Ni Analysis

Leaf samples and quadruplicate portions of 50 μL of protoplast suspensions and 100 μL of vacuole suspensions were dried in a heating block at 100°C and digested for liquid scintillation counting as described previously (Krämer et al., 1997). The Ni content of plant samples used for x-ray absorption spectroscopy was analyzed as follows. Plant samples were dried at 60°C for 3 d, and then digested at 180°C for 105 min in 5 mL of concentrated nitric acid. Samples were cooled to room temperature, 1 mL of 30% (w/v) hydrogen peroxide was added, the mixture was heated at 180°C for 20 min, cooled, and deionized water added to a final volume of 12.5 mL. Ni concentrations were then measured using inductively coupled plasma emission spectroscopy (ICP) (Accuris, Fisons Instruments, Beverly, MA). Certified National Institute of Standards and Technology plant (peach leaf) standards were carried through the digestions and analyzed as part of the quality assurance/quality control protocol. Reagent blanks and spikes were used where appropriate to ensure accuracy and precision in the analysis.

Chlorophyll Determinations

Chlorophyll concentrations in tissue extracts, protoplasts, and vacuole-enriched fractions were estimated according to the method of Strain et al. (1971).

Tissue Extracts

Frozen leaf samples were ground with a pestle and mortar and thawed in 50 mL of phosphate buffer (25 mM potassium phosphate buffer, pH 7.4, and 10 mM dithiothreitol [DTT]) per gram fresh biomass.

Enzyme Assays

Tissue extracts and protoplast and vacuole suspensions were diluted with phosphate buffer (25 mM potassium phosphate and 10 mM DTT) where appropriate, adjusted to a DTT concentration of 10 mM, sonicated (four times for 30 s), and centrifuged at 4°C for 5 min at 12,000*g*. α-Mannosidase activities were determined in the supernatant essentially as described in Vögeli-Lange and Wagner (1990) after pre-incubation in the absence of substrate for 30 min. Acid phosphatase activities were determined using the same protocol, a pre-incubation time of 15 min, *p*-nitrophenylphosphate as a substrate, and an incubation time of 15 min. Under the assay conditions, the extinction coefficient for the product *p*-nitrophenol was determined to be $\epsilon = 18.19\ mM^{-1}\ cm^{-1}$ (data not shown).

NADH-dependent malate dehydrogenase activity was determined in protoplast and vacuole suspensions containing 10 mM DTT after sonication as described above and centrifugation at 4°C and 16,000*g* for 5 min. Fifty microliters of supernatant was added to 1.45 mL of a solution containing 90 mM potassium phosphate, pH 7.4, 0.2 mM oxaloacetic acid, and 0.26 mM NADH. The decrease in A_{340} was followed for 2 min (Vögeli-Lange and Wagner, 1990).

Cytochrome *c* oxidase activities were determined in protoplast and vacuole suspensions in the absence of DTT after sonication as described above and centrifugation at 1,000*g* for 5 min according to the method of Storrie and Madden (1990). Samples heated to 100°C for 5 min were used as blanks in all enzyme assays. All enzyme assays were carried out in triplicate.

Isolation of Protoplasts

After harvest leaves were immediately floated on 10 mL of autoclaved washing buffer containing 500 mM mannitol, 2 mM potassium phosphate, pH 6.0, 1 mM $CaCl_2$, 0.25 mM $Ni(NO_3)_2$, and 0.5 mM $MgCl_2$ in a Petri dish. The abaxial epidermis was stripped from leaves of *T. goesingense*, and all leaves were feathered by applying parallel cuts from the midrib to the edges of the leaves at approximately 1-mm distance. For digestion, leaves were placed with the abaxial side down in Petri dishes (1 g of leaf material per dish) containing 10 mL of washing buffer supplemented with 0.05% (w/v) bovine serum albumin, 0.5 mM DTT, 2% (w/v) Cellulysin (Calbiochem, San Diego), and 0.05% (w/v) pectolyase Y-23 (Seishin Pharmaceutical, Tokyo). Digestion of cell walls was carried out for 8 h in the light (1,600 lux) at 25°C with gentle shaking at 30 rpm. Ten milliliters of digest were filtered through a 114-μm nylon mesh and rinsed twice with 5 mL of washing buffer. For protoplast purification approximately 3.5 mL of filtrate was layered onto 1.5 mL of washing buffer containing 20% (w/v) Ficoll (type 400, Sigma Chemical Co., St. Louis) in a glass centrifuge tube. The gradient was centrifuged in a swinging bucket rotor at approximately 6*g* for 20 min. The protoplasts were collected from the interface with a pasteur pipette and mixed gently with 2 mL of washing buffer containing 20% (w/v) Ficoll (type 400), and the suspension was overlaid first with 1.5 mL of washing buffer containing 14% (w/v) Ficoll (type 400) and subsequently with 1.25 mL of washing buffer. The gradient was centrifuged at 6*g* for 35 min. Protoplasts were collected at the 0%/14% Ficoll interface, suspended gently in 15 mL of washing buffer and centrifuged at 6*g* for 15 min. The supernatant was then removed, and protoplasts were suspended in washing buffer to obtain a protoplast suspension of 1×10^6 to 1.5×10^6 protoplasts per milliliter, as determined by quadruplicate counting of aliquots on a hemacytometer. Aliquots of this suspension were used for the preparation of vacuoles and for the quantification of Ni and chlorophyll, and stored at −20°C for the determination of marker enzyme activities.

Chlorophyll content and marker enzyme activities in whole leaf extracts and in the suspension of purified protoplasts are given in Table I. To determine the proportion of whole leaf Ni or enzyme activity localized in the protoplasts, concentrations and enzyme activities were normalized to the concentration of chlorophyll in the respective fraction. Since all of the chlorophyll is localized in the leaf symplasm, determination of leaf and protoplast chlorophyll can be used to determine the number of cells per unit fresh biomass. If the ratio of an enzymatic activity to chlorophyll concentration was the same in leaf extract and protoplast suspension, localization of this activity would be concluded to be 100% symplasmic.

The marker enzymes used were cytochrome *c* oxidase activity (predominantly mitochondrial) and NADH-dependent malate dehydrogenase activity (predominantly cytoplasmic; Wagner, 1987). Activities of the hydrolytic enzymes acid phosphatase and α-mannosidase were also determined in whole leaves, protoplasts, and vacuole-enriched fractions (data not presented). In *T. goesingense*, about 60% of both the total acid phosphatase and α-mannosidase activity were concluded to be localized in the apoplast, using chlorophyll content as a reference (data not shown). In *T. arvense*, about 20% of the acid phosphatase and about 50% of the α-mannosidase activity were localized in the apoplast (data not shown).

Isolation of Vacuoles

To achieve the release of intact vacuoles, a protocol was used in which protoplasts were subjected to a gentle osmotic shock in combination with a pH increase in the medium and low concentrations of a mild detergent (Wagner and Siegelman, 1975). The isolation of vacuoles was

Table I. *Chlorophyll content and enzyme activities in leaf extracts and protoplast suspensions from plants exposed to 1 μM Ni for 1 d*

Values are means calculated from the results of three independent experiments. The proportions of enzymatic activities localized in the protoplasts were calculated by normalizing enzyme activities to the chlorophyll concentration in the respective fraction. n.d., Not determined.

Plant	Chlorophyll		Enzymatic Activity					
	Whole Leaf	Protoplast	Cytochrome *c* Oxidase			NADH-MDH[a]		
	mg g^{-1}	*μg per 10^6 protoplasts*	*μmol min^{-1} g^{-1}*	*μmol min^{-1} per 10^6 protoplasts*	*% of leaf total*	*μmol min^{-1} g^{-1}*	*μmol min^{-1} per 10^6 protoplasts*	*% of leaf total*
T. goesingense	1.66	62.5	n.d.	0.016	–	144.2	6.7	123
T. arvense	1.21[b]	49.8	n.d.	0.045	–	95.6	4.2	106

[a] MDH, Malate dehydrogenase. [b] Given value is the average from two experiments.

carried out according to a modified protocol based on Vögeli-Lange and Wagner (1990). All steps were carried out on ice or at 4°C. For gentle lysis of protoplasts, 1.5 mL of protoplast suspension was added to 6 mL of ice-cold lysis medium containing 344 mM mannitol, 0.75 mM 3-[(3-cholamidopropyl)dimethylammonio]-1-propanesulfonic acid (CHAPS) (Sigma Chemical Co.), 25 mM 4-(2-hydroxyethyl)-1-piperazineethanesulfonic acid (HEPES)-Tris, pH 8.0, and 1.25 mM EGTA. The suspension was gently stirred with a toothpick for 10 min. Aliquots of 1.25 mL of the lysed protoplast suspension were dispensed into 15-mL disposable glass centrifuge tubes and mixed gently with 2.1 mL of a solution containing 500 mM mannitol, 1 mM EGTA, 0.5 mM CHAPS, 20 mM HEPES-T, pH 8.0, and 20% (w/v) Ficoll (type 400). Ten microliters of a 0.3% (w/v) solution of neutral red in water was added to one of the tubes to monitor the position of the vacuoles in the density gradient. The mixture was carefully overlaid first with 1.25 mL of a solution containing 475 mM mannitol, 0.2 mM CHAPS, 20 mM HEPES-Tris, pH 8.0, and 10% (w/v) Ficoll (type 400), and then with 1.25 mL of a solution containing 475 mM mannitol, 0.2 mM CHAPS, and 20 mM HEPES-Tris. The gradient was centrifuged for 30 min at 650*g*.

Vacuoles were collected at the 0%/10% Ficoll interface and quadruplicate aliquots counted immediately using a hemacytometer after addition of neutral red. Aliquots of this vacuole suspension were immediately sampled for the quantification of ^{63}Ni and chlorophyll or stored at −20°C for the determination of marker enzyme activities. Aliquots were taken from all phases of the gradient and analyzed for Ni and α-mannosidase activities. There was no significant difference in either Ni concentration (averaging 6% of Ni in vacuole-enriched fraction) or α-mannosidase activity (averaging 10% of the activity in vacuole-enriched fraction) between the 0% Ficoll phases of gradients for *T. arvense* and *T. goesingense* ($P = 0.39$ and 0.74, respectively). This suggests that any difference in vacuolar Ni concentrations between the two species was not due to differential leakage of vacuolar contents.

The yield of intact vacuoles was determined by staining with neutral red to improve visibility and quadruplicate visual counting of structures under the light microscope using a hemacytometer. The red color of the vacuoles after neutral red staining indicated that they were able to maintain a low inside pH at a pH of 8.0 in the medium, suggesting that the vacuolar membranes were sealed against net proton leakage. The total number of protoplasts lysed and vacuoles recovered were calculated by taking into account the volume of protoplast suspension lysed and the volume of vacuole suspension recovered, respectively. Based on these values, vacuolar yield and contamination were determined as shown in Table II, assuming that one vacuole was released per protoplast. Vacuole yield can also be quantified by determining the activities of marker enzymes whose subcellular localization is supposed to be limited to the vacuole, i.e. acid phosphatase and α-mannosidase (Vögeli-Lange and Wagner, 1990). This method of vacuole quantification proved inappropriate, because in *T. goesingense* it resulted in nominal vacuole yields of 36% to 40% based on enzyme activity, indicating an inhibition of the hydrolytic enzymes in the protoplast fraction, possibly by a cytoplasmic compound. This was not observed in *T. arvense*.

X-Ray Absorption Spectroscopy

Samples for x-ray absorption spectroscopy were mounted in 1-mm pathlength lucite sample holders with mylar windows. To minimize breakdown and mixing of cellular components within the plant material, care was taken to keep the tissue frozen at all times prior to measurement. To this end, frozen plant tissues were carefully ground under liquid nitrogen and compacted into liquid-nitrogen-cooled cells. Aqueous models were diluted by 30% to 50% (v/v) with glycerol (to avoid ice crystal formation) before being pipetted into holders and rapidly frozen in liquid nitrogen. During data collection, samples were held at a temperature of approximately 15 K using a flowing liquid helium cryostat.

X-ray absorption spectroscopy was carried out on beamline 7-3 of the SSRL using a Si(220) double crystal monochromator, 1-mm upstream vertical aperture, and no focusing optics. Incident intensity was measured using a nitrogen-filled ion chamber, and the absorption spectrum was collected in fluorescence mode using a 13-element germanium detector by monitoring the Ni K_α fluorescence line at 7,472 eV. Spectra were energy calibrated with respect to a spectrum of Ni foil, collected simultaneously with the spectrum of each sample, the first energy-inflection of which is assumed to be 8,333 eV.

Table II. *Vacuolar yield and purity of vacuole-enriched fraction*

No. of vacuoles, chlorophyll content, and marker enzyme activities were determined in the vacuole-enriched fraction, and these values are expressed as a percentage of the respective values measured in the total volume of protoplast suspension lysed to obtain the vacuoles. Values are means of all experiments ± SE.

Plant	No. of Counted Vacuoles	Chlorophyll Content	NADH-MDH[a]	Cytochrome *c* Oxidase Activity
		% of lysed protolasts		
T. goesingense	22.2 ± 1.5	1.2 ± 0.1	2.0 ± 0.4	7.8 ± 4.3
T. arvense	22.1 ± 4.3	0.9 ± 0.5	2.2 ± 0.3	7.7 ± 6.0

[a] MDH, Malate dehydrogenase.

X-ray absorption spectroscopy data reduction was carried out using the EXAFSPAK suite of programs (George, 1998) according to standard methods (Koningsberger and Prins, 1988). Quantitative edge fitting analysis was performed using the program DATFIT (George et al., 1991), in which the near-edge spectrum of the plant material is fit using a least-squares algorithm to obtain a linear combination of edge spectra from a library of Ni model compounds. The fractional contribution of each model spectrum to the fit is then directly proportional to the percentage of Ni chelated by the respective compound in the plant material.

RESULTS

To investigate the subcellular localization of Ni in leaves of *T. goesingense* and *T. arvense*, we used two complementary experimental approaches. The first approach was to obtain intact vacuoles through gentle lysis of leaf protoplasts isolated from plants exposed to radiolabeled Ni. Ni was quantified by liquid scintillation counting in whole leaf, protoplast, and vacuole-enriched fractions and normalized to suitable markers to calculate the subcellular distribution of Ni. The second approach was the use of x-ray absorption spectroscopy to analyze the ligand environment of Ni. This technique is attractive because fractionation or extraction of the plant tissue is unnecessary, minimizing the risk of artifactual changes in the chelation of Ni. Based on standard compounds—Ni bound to cell wall material, a vacuolar type of ligand, or three cytoplasmic ligand types including a sulfur-containing ligand—the localization of Ni was modeled mathematically by obtaining the best fit of the measured spectra out of all possible combinations of standard spectra. A similar procedure was recently used to quantify As, Cd, Se, and Zn ligands in *Astragalus bisulcatus*, *Brassica juncea*, and *Thlaspi caerulescens* (Salt et al., 1995, 1997, 1999; Orser et al., 1999; Pickering et al., 1999; Pickering et al., 2000).

Quantification of Ni in Whole Leaf Tissue, Protoplasts, and Vacuoles

After exposure to Ni, leaves were harvested and cell walls digested enzymatically to obtain protoplasts, which were subsequently purified by centrifugation in a density gradient. Intact protoplasts were sampled and quantified by visual counting under the microscope. Marker enzyme activities and chlorophyll contents were determined in leaf extracts and leaf protoplast solutions (Table I). To obtain vacuoles, protoplasts were gently lysed by exposure to a combination of moderate osmotic stress, an increase in pH, and a mild detergent for 10 min (Wagner and Siegelmann, 1975). This and all subsequent steps were carried out at 4°C to minimize any carrier-mediated efflux from vacuoles. After lysis, the osmotic potential of the medium was increased to stabilize the vacuoles, and vacuoles were purified by centrifugation in a density gradient optimized for purity and recovery of intact vacuoles. Recovery of vacuoles was approximately 22% (Table II). Contamination of the vacuole-enriched fraction with NADH-dependent malate dehydrogenase activity and chlorophyll was low. However, there was highly variable contamination with cytochrome *c* oxidase activity (between 0.6% and 20%) averaging between 8% and 10%, suggesting the presence of mitochondrial membranes in the vacuole-enriched fraction. The extent of this contamination showed no correlation with the amounts of Ni detected in the vacuolar fraction, suggesting that the contaminating mitochondrial membranes did not introduce significant amounts of Ni into the vacuole-enriched fraction.

Total leaf, protoplast, and vacuolar Ni showed considerable variability between replicate experiments (Table III). The percentage of protoplast Ni localized in the vacuole-enriched fractions and the percentage of leaf Ni localized in the protoplast-enriched fractions were calculated separately for each of the three replicate experiments performed for one exposure regime/species combination and then

Table III. *Nickel content in leaf tissue, leaf protoplasts, and leaf vacuoles of T. goesingense and T. arvense*
Values are means of three experiments ± SD.

	Leaf Ni	Protoplast Ni	Vacuolar Ni	
	nmol g^{-1} fresh biomass	*nmol per 10^6 protoplasts*	*nmol per 10^6 vacuoles*	*% total protoplast Ni*[a]
T. goesingense				
1 week of Ni exposure (10 μM Ni)	613 ± 337	8.6 ± 4.1	6.0 ± 2.4	74.7 ± 18.4
1 d of Ni exposure (1 μM Ni)	15.6 ± 5.6	0.23 ± 0.05[b]	0.11 ± 0.01[b]	52.7 ± 8.7[c]
T. arvense				
1 d of Ni exposure (1 μM Ni)	18.6 ± 11.1	0.24 ± 0.17	0.05 ± 0.01	25.4 ± 12.4[c]

[a] Because total leaf and protoplast Ni showed considerable variability between replicate experiments and thus individual plants (see "Material and Methods") the percentage of Ni localized in the vacuole-enriched fraction in each independent replicate experiment ($n = 3$) was calculated and used to derive a mean ± SD for the exposure regime or species, respectively. [b] Values represent mean ± SD of two independent experiments; the third experiment was not included in the mean as it represented a clear outlier (leaf, and thus protoplast and vacuolar Ni concentration were found to be unusually low; Krämer et al., 1997). However, the percentage localization of Ni between the protoplast and vacuole was similar in all three experiments and therefore all the percentage data was included in the mean and used in the t-test (see footnotes a and c). [c] Values significantly different (*t* test, $P < 0.05$).

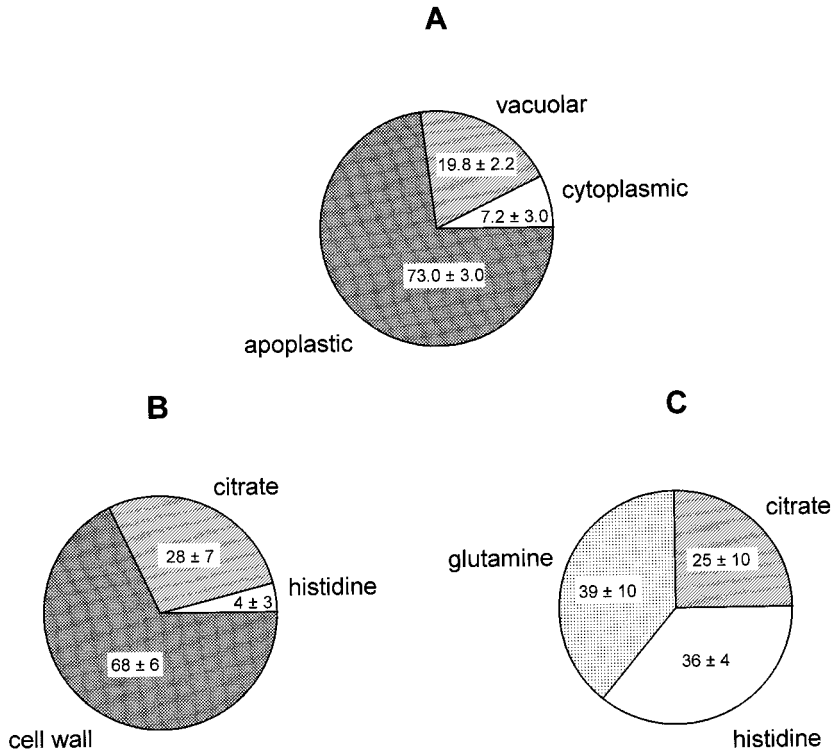

Figure 1. Subcellular localization and speciation of Ni in leaves of hyper- and non-accumulator *Thlaspi* species as a percentage of total leaf Ni. Plants were exposed to 10 μM Ni in a hydroponic solution for 7 d. Leaf samples were collected and used for protoplast and vacuole isolation (A) or analyzed for Ni speciation using x-ray absorption (B). A, Subcellular localization of Ni in *T. goesingense* as determined by cell fractionation. For each independent replicate experiment, leaf Ni concentrations (as nmol g^{-1} fresh biomass) and protoplast Ni concentrations (as Ni per 10^6 structures; primary data as summarized in Table III) were normalized to chlorophyll contents. Ni in the protoplast fractions was calculated as a percentage of total leaf Ni, and the remainder of leaf Ni was concluded to be localized in the apoplast. Ni contents of the vacuolar fractions of the protoplasts were calculated based on the assumption that one vacuole was released per protoplast, and are expressed as a percentage of total leaf Ni. The remainder of the protoplast Ni was concluded to be localized in the cytoplasm. Values are averages of percentages calculated individually for three independent replicate experiments ± SD. B, Major Ni species present in *T. goesingense* as determined by x-ray absorption spectroscopy. Values represent the percentage of total leaf Ni associated with each ligand ± 95% confidence limit. Total leaf Ni was 501 nmol g^{-1} fresh biomass. C, Major Ni species present in *T. arvense* as determined by x-ray absorption spectroscopy. Values represent the percentage of total leaf Ni associated with each ligand ± 95% confidence limit. Total leaf Ni was 310 nmol g^{-1} fresh biomass. X-ray absorption data were collected from a single representative plant sample for each species and each x-ray spectrum used for the fits represents the mean of three independent scans, each being composed of data acquired from 13 independent detectors.

averaged (Table III; Fig. 1A), resulting in a much lower variability between replicate experiments. This suggests that between replicate experiments—and thus between individual plants analyzed—there was considerable variability in leaf Ni concentration, but much less variability in the relative distribution of the metal in the leaf between vacuole, cytoplasm, and apoplast. After 1 week of exposure of *T. goesingense* to 10 μM Ni, 74.7% ± 18.4% of the Ni associated with the protoplast fraction was recovered in the vacuole-enriched fraction (calculated from primary data as summarized in Table III), indicating that the leaf vacuole is the major compartment for the intracellular detoxification of Ni in the hyperaccumulator. At the whole-leaf level, a high proportion of total leaf Ni was found to be localized in the apoplast (73.0% ± 3.0% or 447 nmol g^{-1} fresh biomass; Fig. 1A). Only about one-fifth of the total leaf Ni was found to be localized in the vacuole (19.8% ± 2.2% or 121 nmol g^{-1} fresh biomass), with only a small fraction localized intracellularly outside the vacuole (7.2% ± 3.0% or 44 nmol g^{-1} fresh biomass; Fig. 1A).

A second experiment was performed to compare Ni localization in the Ni-tolerant hyperaccumulator *T. goesingense* and the non-tolerant non-accumulator *T. arvense*. Because *T. arvense* is considerably less tolerant to Ni than *T. goesingense*, we used only 1 μM Ni in the hydroponic medium, and an exposure period of 1 d. Under these conditions, no reduction in evapotranspiration, a common symptom of Ni toxicity, was observed in the non-tolerant *T. arvense* (Krämer et al., 1997). In this experiment, 52.7% ± 8.7% of the protoplast Ni was localized in the vacuoles of the hyperaccumulator, whereas a significantly smaller proportion, 25.4% ± 12.4% of the protoplast Ni was vacuolar in the non-accumulator *T. arvense* ($P < 0.05$; three experiments for each species; calculated from primary data as summarized in Table III).

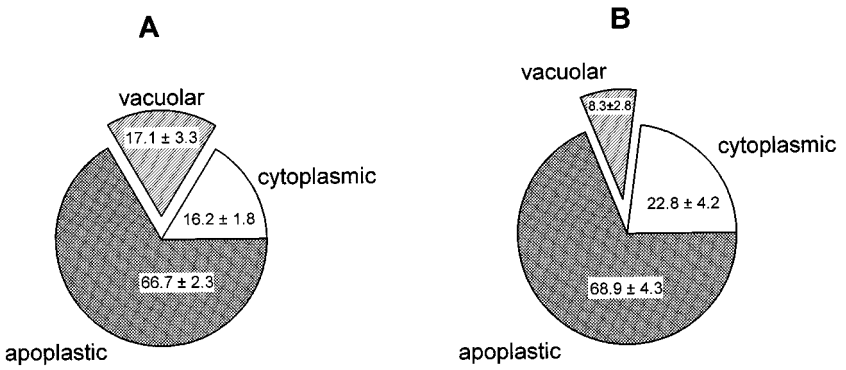

Figure 2. Subcellular localization of Ni in leaves of hyper- and non-accumulator *Thlaspi* species as a percentage of total leaf Ni. Plants were exposed to 1 μM Ni (containing 40 μCi ^{63}Ni per μmol Ni) in a hydroponic solution for 1 d. Leaf samples were collected and fractionated into protoplasts and intact vacuoles. Ni localization was calculated as described in Figure 1. Values were averaged from three independent experiments ± SD. A, Subcellular distribution of Ni in *T. goesingense*. B, Subcellular distribution of Ni in *T. arvense*.

Despite the differences in vacuolar localization between the two species, their leaves contained approximately equal concentrations of Ni (Table III) after 1 d of exposure to 1 μM Ni. This is in agreement with our earlier findings that in the absence of Ni toxicity, the rate of shoot Ni accumulation is the same in *T. arvense* and in *T. goesingense* (Krämer et al., 1997). The amount of Ni in protoplasts was also approximately equivalent in the two species (Table III), indicating that transport of Ni through the plasma membrane does not occur at an elevated rate in the hyperaccumulator *T. goesingense*. The proportion of Ni localized in the apoplast was also similar in the two species (66.7% ± 2.3% and 68.9% ± 4.3%, respectively; Fig. 2). Therefore, at the whole-leaf level the only difference between the two species was the Ni content of the vacuoles, which was 2-fold higher in *T. goesingense* (17.1% ± 3.3%) than in *T. arvense* (8.3% ± 2.8%; Fig. 2).

Quantitative Speciation of Ni in Whole Shoot Tissue

The near-edge x-ray absorption spectrum of Ni is sensitive to the molecular environment of the Ni^{2+} central cation, as demonstrated in Figure 3. Figure 3A compares the spectrum of aqueous Ni^{2+} with those of Ni in solution chelated to citrate, His, or a sulfur ligand. In the presence of excess His and at neutral pH, Ni is coordinated by two His molecules through both neutral ring and amino nitrogens and the weakly interacting negative carboxyl oxygen to form $Ni(His)_2$ (Sundberg and Martin, 1974). In contrast, citrate chelates Ni through the hydroxyl and carboxyl oxygens. The resulting differences in the coordination geometry between the two ligands are exemplified in their x-ray absorption near-edge spectra (Fig. 3A). For comparison, the spectrum of the sulfur-containing compound $[Ni(SPh)_4]^{2-}$ (Eidsness et al., 1989) is also shown; in this compound the Ni is coordinated by four sulfur ligands and the resulting spectrum shows substantial differences. The near-edge spectrum is also sensitive to more subtle differences in local coordination (Fig. 3B).

Therefore, although the spectra of Ni coordinated to Gln or cell wall are broadly similar to those of aqueous Ni^{2+} or Ni-citrate, there are features in each of these spectra that could be diagnostic in identifying these in a mixture (within certain limits). In this way, the citrate spectrum has a more pronounced feature between 8360 and 8370 eV than do the others, and the aqueous Ni^{2+} has a more pronounced main peak with a rising edge to marginally higher energy. The near-edge spectra of shoots of *T. goesingense* and *T. arvense* are shown in Figure 4. It can be seen that, whereas the major peak is more intense in *T. goesingense*, the broad feature at 8360 to 8370 eV is similar for the two species. The best fit of the spectra of *T. goesingense* and *T. arvense* tissues (Fig. 5), using a linear combination of spectra of standard compounds, provided information on the likely identity of the endogenous Ni ligands in these tissues.

After exposure to 10 μM Ni for 7 d, 68% ± 6% (±95% confidence limit) of Ni in shoots of *T. goesingense* was found to be chelated by cell wall material (Fig. 1B), a smaller proportion was found to be chelated by citrate (28% ± 7%), and a very small fraction by His (4% ± 3%). In contrast, Ni chelated by Gln and His constituted the major species in shoots of the non-accumulator *T. arvense* (39% ± 10% and 36% ± 4%, respectively), with Ni-citrate comprising the rest (25% ± 10%; Fig. 1C). Comparison of Figure 1, A and B, indicates a striking similarity between the proportional localization of Ni and its proportional speciation between ligand types in *T. goesingense*. The proportions of Ni found to be localized in the apoplast after the isolation of protoplasts (Fig. 1A) and the proportions found to be bound to cell wall material were identical within the precision of the edge fits (Fig. 1B). Thus, Ni binding by cell wall material appeared to correspond to apoplastic Ni, indicating that there was no significant leakage of Ni from protoplasts during the fractionation process. Chelation by citrate and His largely corresponded to vacuolar and extravacuolar localization within the cell, respectively, and these values are also identical within the margins of error of the analysis. The speciation of Ni in *T. arvense* suggests that a major proportion, more than 70% (Ni coordinated by Gln and His), was localized in the cytoplasm (Fig. 1C). However, this could not be confirmed by cell fractionation, since exposure of *T. arvense* to 10 μM Ni for 1 week resulted in severe Ni toxicity.

X-ray absorption spectroscopic studies were not performed on shoot tissue isolated from plants exposed to 1 μM Ni for 1 d because of the low shoot Ni concentrations these plants contained (Table III). We have therefore not been able to determine the speciation of Ni in these plants. Increases in the sensitivity of the x-ray absorption instru-

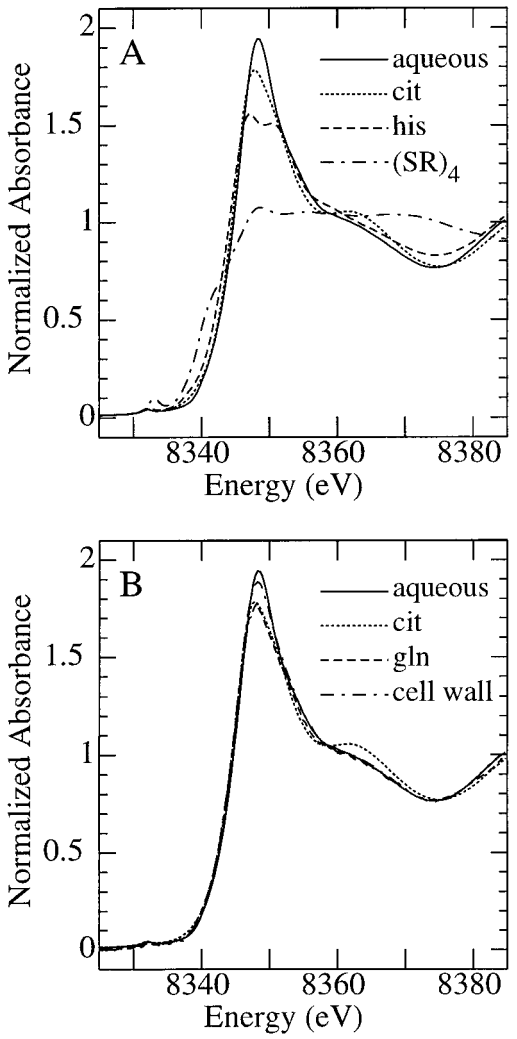

Figure 3. X-ray absorption near-edge spectra of selected aqueous Ni species recorded at the Ni K-edge. The order of spectra plotted at the edge, from top to bottom, is as follows: A, Aqueous Ni^{2+} (6.66 mM $Ni[NO_3]_2$, pH 7.0), Ni-citrate (6.66 mM $Ni[NO_3]_2$ and 70 mM citrate, pH 8.0), Ni-His (6.66 mM $Ni[NO_3]_2$ and 80 mM His, pH 7.0), and $(Ni[SPh]_4^{2-}$; Eidsness et al., 1989). B, Aqueous Ni^{2+} (6.66 mM $Ni[NO_3]_2$, pH 7.0), isolated *T. goesingense* shoot cell wall material (Lasat et al., 1996), Ni-citrate (6.66 mM $Ni[NO_3]_2$ and 70 mM citrate, pH 8.0), and Ni-Gln (1 mM $Ni[NO_3]_2$ and 4 mM Gln, pH 7.3).

mentation at the SSRL should facilitate these experiments in the future.

DISCUSSION

Previous studies have concluded that the pronounced Ni tolerance of *T. goesingense* appears to be sufficient to explain the Ni hyperaccumulation phenotype observed in hydroponic culture (Krämer et al., 1997). At Ni concentrations where this Ni tolerance mechanism was operating in *T. goesingense* (10 μM Ni exposure for 7 d) about 75% of the intracellular leaf Ni was found to be localized in the vacuole (Table III; Fig. 1). Using x-ray absorption spectroscopy to analyze the speciation of Ni in leaf tissues, and following an identical Ni exposure protocol, we found that 87% of the Ni not bound to the cell wall was chelated by citrate (Fig. 1B). This is very similar to, and within the observed variability of, the amount of Ni found to be localized in the vacuole. The vacuole is known to be the predominant location for storage of organic acids such as citrate and malate in the cell (Ryan and Walker-Simmons, 1983). It is also known that citrate is able to effectively chelate Ni at the acidic pH of the vacuole (Dawson et al., 1986). Our data are therefore consistent with the hypothesis that vacuolar storage of Ni, predominantly in the form of a Ni-organic acid complex, plays an important role in the Ni tolerance of the hyperaccumulator.

Approximately 25% of intracellular Ni in the leaves of *T. goesingense* was found to be extravacuolar (Fig. 1A). X-ray absorption spectroscopy (Fig. 1B) indicated that a small but significant fraction of the total Ni present is bound to His, equivalent to up to 25% of the intracellular Ni. The data provide evidence that free His, or some other His-like ligand may be involved in shuttling Ni across the cytoplasm for loading into the vacuole in a manner similar to that proposed for Ni loading into the xylem in Ni-hyperaccumulating *Alyssum* species (Krämer et al., 1996). Due to the high stability constant of the Ni-His complex and the protonation constants of His, this amino acid is an ideal chelator of Ni at the pH values commonly found in the cytoplasm (pH approximately 7.5). However, at the low pH values of the vacuole (pH approximately 5.5) the imidazole nitrogen of His becomes protonated. This results in a decrease of the apparent stability constant of the Ni-His complex, favoring the coordination of Ni by organic acids including citrate. Ni coordination by sulfur ligands was not observed in any of the x-ray absorption spectra, confirming that phytochelatins are not involved in Ni binding in either the hyper- or non-accumulator species of *Thlaspi* studied.

If, as we propose, the non-accumulator *T. arvense* has only a limited capacity for vacuolar storage of Ni, we might

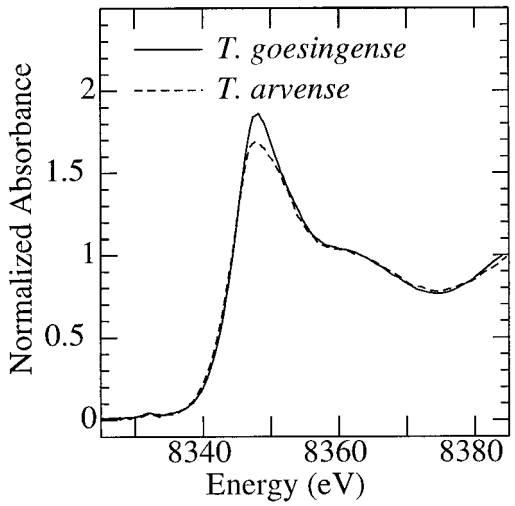

Figure 4. Ni K-edge x-ray absorption near-edge spectra of shoots of *T. goesingense* (solid line) and *T. arvense* (broken line). Plants were grown hydroponically and exposed to 10 μM Ni for 7 d before harvest.

expect Ni to accumulate in the cytoplasm of this species. In the neutral pH environment of the cytoplasm, we would expect Ni to bind to ligands containing nitrogen, oxygen, and sulfur, such as His, Gln, and Cys moieties in proteins, free amino acids, glutathione, and various nucleotides (Dawson et al., 1986). A high degree of non-specific binding of Ni to these important biomolecules in the cell would lead to toxicity and cell death. Indeed, after exposure of the non-accumulator *T. arvense* to toxic concentrations of Ni (10 μM Ni exposure for 7 d), 36% of the accumulated Ni was chelated to His-like ligands (Fig. 1C), substantially more than in *T. goesingense* under the same conditions (Fig. 1B). A significant proportion of Ni was also observed to be chelated with Gln-type ligands, a Ni complex not observed in the hyperaccumulator *T. goesingense*. These ligands only effectively coordinate Ni at the near-neutral pH of the cytoplasm (Dawson et al., 1986), a fact we confirmed using x-ray absorption spectroscopy (data not shown). Thus, the presence of these Ni complexes in the non-accumulator *T. arvense* supports the hypothesis that Ni accumulates in the cytoplasm of the non-accumulator, thereby poisoning sensitive cellular processes and ultimately causing cell death.

A similar conclusion was also drawn for barley exposed to Ni (Brune et al., 1995). After 1 d, cytoplasmic Ni is already higher in *T. arvense* than in *T. goesingense* (Fig. 2). Therefore, it is possible that the speciation of Ni observed in *T. arvense* after 7 d is a consequence of cellular damage, possibly pH increases in the vacuole or in the apoplast, which could favor Ni binding by Gln or Gln-type ligands, or even cell lysis. The hyperaccumulator *T. goesingense* is apparently able to avoid this by continuously and efficiently storing Ni in the vacuole, where the metal ion appears to be coordinated mainly with citrate (Fig. 1, A and B). Vacuolar metal accumulation has also been observed in the Zn hyperaccumulator *T. caerulescens* using electron microscopy and x-ray microanalysis (Vazquez et al., 1992, 1994). In this hyperaccumulator, shoot Zn has been shown to be present mainly as the hydrated cation, and is coordinated to citrate and oxalate (Salt et al., 1999).

By directly comparing the Ni contents of vacuoles from the hyperaccumulator *T. goesingense* and the non-accumulator *T. arvense*, we have been able to confirm that *T. goesingense* can more efficiently compartmentalize Ni in the vacuole (Table III; Fig. 2). At low concentrations of Ni, conditions under which leaf and protoplast Ni concentrations were equivalent in both species and *T. arvense* was not suffering any Ni toxicity, vacuoles of *T. goesingense* contained twice as much Ni as vacuoles of *T. arvense* (Table III). Similarly, in *T. goesingense* vacuolar Ni was about twice as high as in *T. arvense* when expressed as a proportion of total leaf Ni (Fig. 2). This suggests that the higher amounts of Ni in the vacuoles of *T. goesingense* were not merely a consequence of a larger vacuolar and thus cellular volume. These results support the contention that differences between the vacuolar Ni concentrations of the two species were due to the presence of a more efficient vacuolar sequestration mechanism for Ni in the hyperaccumulator.

An alternative explanation for the observed difference in vacuolar Ni contents between *T. goesingense* and *T. arvense* could be that vacuoles from the two *Thlaspi* species lost Ni at different rates during the isolation process. However, several lines of evidence mitigate this suggestion. The densities of the purification gradient were designed to cause the vacuoles to migrate up through the gradient and collect at the 0%/10% Ficoll interface. Unaided, soluble Ni and α-mannosidase were unable to migrate in this way (diffusion would be insignificant under these conditions). Therefore, the Ni and α-mannosidase activity measured in the upper 0% Ficoll phase most likely represented material that had leaked from vacuoles collected at the 0%/10% Ficoll interface. The upper phase (0% Ficoll) of the vacuolar purification gradient was found to contain only 6% to 10% of the concentration of Ni and α-mannosidase activity found in the vacuolar-enriched fraction. However, in this upper phase, no significant difference was found in either Ni

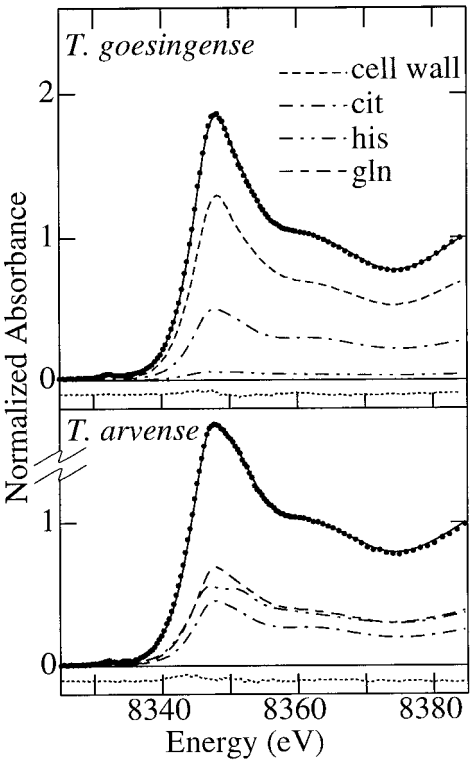

Figure 5. Results of quantitative modeling of x-ray absorption near-edge spectra obtained from shoots of *T. goesingense* and *T. arvense*. The spectrum of a mixture of Ni complexes is the sum of the spectra of all constituent complex species scaled by their relative proportional contribution to overall Ni chelation. By fitting spectra of aqueous Ni, Ni coordinated with His (6.66 mM $Ni[NO_3]_2$, 80 mM His, and 30% [v/v] glycerol, pH 7.0), citrate (6.66 mM $Ni[NO_3]_2$, 70 mM citrate, and 30% [v/v] glycerol, pH 8.0), Gln (1 mM $Ni[NO_3]_2$, 4 mM Gln, and 30% [v/v] glycerol, pH 7.3), and isolated *T. goesingense* shoot cell wall material (Lasat et al., 1996), we were able to determine the relative contribution of each compound as a ligand of Ni in planta (Fig. 1). A, *T. goesingense* shoots; relative goodness of fit of 0.06×10^{-3}. B, *T. arvense* shoots; relative goodness of fit of 0.1×10^{-3}. The figure shows the data (points), the best fit (solid line) and the residual (dotted line), together with the individual fractional contributions. The goodness of fit is defined as $\Sigma[(I_{obsd.} - I_{calcd.})^2]/n$, where n is the number of points in the spectrum and $I_{obsd.}$ and I_{calcd} are the observed and calculated points, respectively.

concentration or α-mannosidase activity between the two *Thlaspi* species. This suggests that vacuolar leak rates are the same in both species.

In support of this conclusion, the vacuolar Ni content of the plants analyzed was found not to correlate with the amount of Ni or α-mannosidase activity observed in the upper phase of the vacuolar purification gradient. Overall, leakage of Ni from protoplasts during their isolation also appeared to be low. The amount of Ni found to be associated with the cell wall using x-ray absorption spectroscopy was very similar to that found to be associated with the apoplast by cellular fractionation (Table III; Fig. 1). Apoplastic Ni was calculated by subtracting protoplast-associated Ni from total leaf Ni. If significant amounts of Ni had leaked from the protoplasts, then the amount of Ni calculated to be associated with the apoplast would have been inflated. Care was also taken to minimize carrier-mediated efflux of Ni from vacuoles by performing lysis and gradient centrifugation at 4°C and by increasing the osmotic potential of the medium after lysis of the protoplasts. Moreover, during and after isolation, vacuoles were found to be tightly sealed, as demonstrated by their stainability with neutral red.

Since protoplast and apoplast Ni contents were similar in the two species (Table III; Fig. 2), Ni exclusion from cells or localization in the apoplast appears to be of little importance for Ni tolerance in the hyperaccumulator species. The absolute amount of Ni localized intracellularly outside the vacuole was found to be about one order of magnitude higher in *T. goesingense* exposed to Ni for 1 week than in the plants exposed for 1 d (Table III; Figs. 1A and 2A). It is therefore possible that, in addition to efficient Ni transport into the vacuole, an as-yet-unidentified cytoplasmic chelator, possibly His, or accumulation in an organelle other than the vacuole, may also contribute to Ni tolerance.

A large proportion of total leaf Ni, between 67% and 73%, was found to be localized in the apoplast or bound to cell wall material (Figs. 1 and 2). This extracellular Ni might represent the occupation of binding sites available in the apoplast or even the replacement of extracellularly bound calcium. Dead cell wall material prepared from *T. goesingense* was found to contain 6,100 nmol g^{-1} dry biomass Ni after incubation in 10 μM Ni for 24 h, suggesting a very high cation binding capacity of this cell wall material (D.E. Salt, unpublished data). Equal amounts of Ni appear to be localized in the apoplast of the hyperaccumulator and non-accumulator under conditions of low-level Ni exposure (Fig. 2). Since the capacity of the cell wall for cation binding is high, the occupation of extracellular binding sites might continue for several days until saturation is reached. Under Ni exposure conditions that are toxic to the non-accumulator (Fig. 1C), the hyperaccumulator appears to have a higher capacity to bind Ni to the cell wall (Fig. 1B) compared with the non-accumulator (Fig. 1, B and C). This may reflect the presence of more cell wall material in the hyperaccumulator or a specific modification of the cell wall matrix to allow increased Ni binding. Alternatively, Ni-induced cellular toxicity in the non-accumulator *T. arvense* may reduce the Ni-binding capacity of the apoplast via a decrease in the apoplastic pH or leakage of competing cations from the cells.

Our data suggest that the ability of the hyperaccumulator *T. goesingense* to efficiently store Ni in vacuoles plays a key role in the previously observed Ni tolerance of leaf protoplasts (Krämer et al., 1997). A Ni storage mechanism efficient enough to prevent metal toxicity appears to be lacking in the Ni-sensitive non-accumulator *T. arvense*. Since Ni tolerance appears sufficient to explain the Ni hyperaccumulation phenotype observed in hydroponically cultured *T. goesingense* (Krämer et al., 1997), we can conclude that vacuolar compartmentalization of Ni in *T. goesingense* plays a major role in the cellular basis of Ni hyperaccumulation in this species. Our future research efforts will address the molecular mechanisms involved in this enhanced vacuolar compartmentalization of Ni in *T. goesingense*.

ACKNOWLEDGMENTS

We would like to thank Dr. Faith Belanger and Dr. Eric Lam for the kind permission to use their microscopic equipment. We are grateful to Graham George of SSRL for helpful discussions

Received October 21, 1999; accepted December 14, 1999.

LITERATURE CITED

Baker AJM, Brooks RR (1989) Terrestrial higher plants which hyperaccumulate metallic elements: a review of their distribution, ecology and phytochemistry. Biorecovery **1:** 81–126

Brune A, Urbach W, Dietz K-J (1994) Compartmentation and transport of zinc in barley primary leaves as basic mechanisms involved in zinc tolerance. Plant Cell Environ **17:** 153–162

Brune A, Urbach W, Dietz K-J (1995) Differential toxicity of heavy metals is partly related to a loss of preferential extraplasmatic compartmentation: a comparison of Cd-, Mo-, Ni-, and Zn-stress. New Phytol **129:** 403–409

Chaney RL (1983) Plant uptake of inorganic waste. *In* JE Parr, PB Marsh, JM Kla, eds, Land Treatment of Hazardous Wastes. Noyes Data, Park Ridge, IL, pp 50–76

Dawson RMC, Elliott DC, Elliott WH, Jones KM, eds, (1986) Data for Biochemical Research, Ed 3. Clarendon Press, Oxford, UK

De Souza MP, Pilon-Smits EAH, Lytle CM, Hwang S, Tai J, Honma TSU, Yeh L, Terry N (1998) Rate-limiting steps in selenium assimilation and volatilization by Indian mustard. Plant Physiol **117:** 1487–1494

Eidsness MK, Scott RA, Prickril B, DerVartanian DV, LeGall J, Moura I, Moura JJG, Peck HD Jr (1989) Evidence for selenocysteine coordination to the active site nickel in the [NiFeSe]-hydrogenase from *Desulfovibrio baculatus*. Proc Natl Acad Sci USA **86:** 147–151

George GN (1998) EXAFSPAK, a suite of programs for x-ray absorption spectroscopy data analysis. http://ssrl.slac.stanford.edu/exafspak.html

George GN, Gorbaty ML, Keleman SR, Sansone M (1991) Direct determination and quantification of sulfur forms in coals from the Argonne premium sample program. Energy Fuels **5:** 93–97

Gries GE, Wagner GJ (1998) Association of nickel versus transport of cadmium and calcium in tonoplast vesicles of oat roots. Planta **204:** 390–396

Koningsberger DC, Prins R (1988) X-Ray Absorption Principles, Applications, Techniques of EXAFS, SEXAFS and XANES. John Wiley & Sons, New York

Krämer U, Cotter-Howells JD, Charnock JM, Baker AJM, Smith JAC (1996) Free histidine as a metal chelator in plants that accumulate nickel. Nature **379:** 635–638

Krämer U, Smith RD, Wenzel WW, Raskin I, Salt DE (1997) The role of metal transport and tolerance in nickel hyperaccumulation by *Thlaspi goesingense* Hálácsy. Plant Physiol **115:** 1641–1650

Krotz RM, Evangelou BP, Wagner GJ (1989) Relationship between cadmium, zinc, Cd-peptide, and organic acid in tobacco suspension cells. Plant Physiol **91:** 780–787

Lasat MM, Baker AJM, Kochian LV (1996) Physiological characterization of root Zn^{2+} absorption and translocation to shoots in Zn hyperaccumulator and nonaccumulator species of *Thlaspi*. Plant Physiol **112:** 1715–1722

Lytle CM, Lytle FW, Yang N, Qian JH, Hansen D, Zayed A, Terry N (1998) Reduction of Cr(VI) to Cr(III) by wetland plants: potential for in situ heavy metal detoxification. Environ Sci Technol **32:** 3087–3093

Nishimura K, Igarashi K, Kakinuma Y (1998) Proton gradient-driven nickel uptake by vacuolar membrane vesicles of *Saccharomyces cerevisiae*. J Bacteriol **180:** 1962–1964

Orser CS, Salt DE, Pickering IJ, Prince R, Epstein A, Ensley BD (1999) *Brassica* plants to provide enhanced human mineral nutrition: selenium phytoenrichment and metabolic transformation. J Med Food **1:** 253–261

Pickering IJ, Prince RC, George MJ, Smith RD, George GN, Salt DE (2000) Reduction and coordination of arsenic in Indian mustard. Plant Physiol **122:** 1171–1177

Pilon-Smits EAH, Hwang S, Lytle CM, Zhu Y, Tai JC, Bravo RC, Chen Y, Leustek T, Terry N (1999) Overexpression of ATP sulfurylase in Indian mustard leads to increased selenate uptake, reduction, and tolerance. Plant Physiol **119:** 123–132

Ramsay LM, Gadd GM (1997) Mutants of *Saccharomyces cerevisiae* defective in vacuolar function confirm a role for the vacuole in toxic metal ion detoxification. FEMS Microbiol Lett **152:** 293–298

Ryan CA, Walker-Simmons M (1983) Plant vacuoles. Methods Enzymol **96:** 580–589

Salt DE, Krämer U (1999) Mechanisms of metal hyperaccumulation in plants. *In* BD Ensley, I Raskin, eds, Phytoremediation of Toxic Metals: Using Plants to Clean-Up the Environment. John Wiley & Sons, New York, pp 231–246

Salt DE, Pickering IJ, Prince RC, Gleba D, Dushenkov S, Smith RD, Raskin I (1997) Metal accumulation by aquacultured seedlings of Indian mustard. Environ Sci Technol **31:** 1635–1644

Salt DE, Prince RC, Baker AJM, Raskin I, Pickering IJ (1999) Zinc ligands in the metal hyperaccumulator *Thlaspi caerulescens* as determined using x-ray absorption spectroscopy. Environ Sci Technol **33:** 713–717

Salt DE, Prince RC, Pickering IJ, Raskin I (1995) Mechanisms of cadmium mobility and accumulation in Indian mustard. Plant Physiol **109:** 427–433

Salt DE, Smith RD, Raskin I (1998) Phytoremediation. Annu Rev Plant Physiol Plant Mol Biol **49:** 643–668

Shrift A (1969) Aspects of selenium metabolism in higher plants. Annu Rev Plant Physiol **20:** 475–495

Storrie B, Madden EA (1990) Isolation of subcellular organelles. Methods Enzymol **182:** 203–225

Strain HH, Cope BT, Svec WA (1971) Analytical procedures for the isolation, identification, estimation, and investigation of the chlorophylls. Methods Enzymol **23:** 452–476

Sundberg RJ, Martin RB (1974) Interactions of histidine and other imidazole derivatives with transition metal ions in chemical and biological systems. Chem Rev **74:** 471–517

Vazquez MD, Barcelo J, Poschenrieder C, Madico J, Hatton P, Baker AJM, Cope GH (1992) Localization of zinc and cadmium in *Thlaspi caerulescens* (Brassicaceae), a metallophyte that can hyperaccumulate both metals. J Plant Physiol **140:** 350–355

Vazquez MD, Poschenrieder C, Barcelo J, Baker AJM, Hatton P, Cope GH (1994) Compartmentation of zinc in roots and leaves of the zinc hyperaccumulator *Thlaspi caerulescens* Bot Acta **107:** 243–250

Vögeli-Lange R, Wagner GJ (1990) Subcellular localization of cadmium and cadmium-binding peptides in tobacco leaves. Plant Physiol **92:** 1086–1093

Wagner GJ (1987) Methodological and other aspects of intact mature higher plant cell vacuoles. *In* B Martin, ed, Plant Vacuoles, Their Importance in Solute Compartmentation in Cells and Their Application in Plant Biotechnology. North Atlantic Treaty Organization Advanced Study Institutes Series. Plenum Press, New York, pp 7–19

Wagner GJ, Siegelman HW (1975) Large-scale isolation of intact vacuoles and isolation of chloroplasts from protoplasts of mature plant tissues. Science **190:** 1298–1299